Water Science & Technology

IWA PUBLISHING

Water Science & Technology Vol 88 No 11, 2917 doi: 10.2166/wst.2023.356

Primary and digested sludge-derived char as a Cd sorbent: feasibility of local utilisation

Ida Sylwan [a,*], Davide Bergna [b], Hanna Runtti [b], Lena Johansson Westholm [a] and Eva Thorin [a]

[a] Mälardalen University, School of Business, Society and Engineering, Future Energy Center, P.O. Box 883, SE-721 23 Västerås, Sweden
[b] Research Unit of Sustainable Chemistry, University of Oulu, P.O. Box 8000, FI-90014 Oulu, Finland
*Corresponding author. E-mail: ida.sylwan@ri.se

IS, 0000-0002-9373-2774; DB, 0000-0001-9479-3563; HR, 0000-0002-2289-1778; LJW, 0000-0003-0231-564X; ET, 0000-0002-3485-5440

ABSTRACT

Cadmium (Cd) is a highly toxic metal, occurring in municipal wastewater and stormwater as well as in wastewater from various industries. Char derived from the pyrolysis of municipal sewage sludge has the potential to be a low-cost sorption media for the removal of Cd. However, the balance between possible local char production and demand has not been assessed previously. In this study, the Cd sorption capacities of chars derived from primary (PSC) and secondary sludge (DSC), as well as the feasibility of char production for Cd sorbent purposes, and the pyrolysis energy balance were evaluated. Results showed that the sorption capacity of PSC (9.1 mg/g; 800 °C, 70 min) was superior to that of DSC (6.0 mg/g; 800 °C, 70 min), and increased with a higher pyrolysis temperature. Pyrolysis of primary sludge had a more favourable energy balance compared with the pyrolysis of digested sludge; however, when accounting for loss of biogas production the energy balance of primary sludge pyrolysis was negative. Assessment of the regional demand (Västerås, Sweden) indicated that PSC or DSC may cover the local Cd sorbent demand. However, it was estimated that large char volumes would be required, thus making the use of DSC/PSC less feasible.

Key words: adsorbent, adsorption, biochar, biosolids, biosorbent

HIGHLIGHTS

- Char derived from the pyrolysis of municipal sewage sludge is a potential low-cost technology for Cd removal.
- Char derived from primary sludge showed superior sorption capacity compared to char derived from mixed digested sludge.
- Theoretical calculations indicated a potentially positive energy balance of digested sludge pyrolysis.
- Locally, sludge pyrolysis may not be motivated by Cd sorbent production alone.

GRAPHICAL ABSTRACT

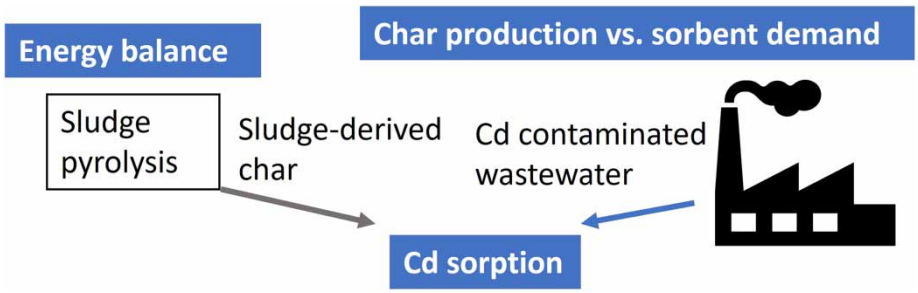

1. INTRODUCTION

Industrialisation has led to increased concentrations of metals in the biosphere, with associated toxicity to humans and ecosystems. Due to its high toxicity, cadmium (Cd) is one of the priority metals of concern (European Commission 2008; Huang *et al.* 2020). Effects of Cd exposure include increased risk of cancer, decreased fertility, and impacts on foetal development (Tchounwou *et al.* 2012). One route to mitigate Cd pollution is wastewater treatment. Cd occurs in a variety of wastewaters, for instance, drainage from mine tailings (Bogush & Voronin 2011), tannery effluents (Arti & Mehra 2023), textile factory

effluents, leachate from landfills and waste management sites (Öman *et al.* 2000), stormwater (especially road runoff and runoff from impermeable surfaces) (Göbel *et al.* 2007), flue gas condensate from combined heat and power plants (CHP) (Noor *et al.* 2020), car wash wastewater (Sörme & Lagerkvist 2002), and municipal wastewater (Choubert *et al.* 2011). A compilation of typical Cd concentrations in various wastewaters is given in Supplementary Material, Table S1. According to this data, concentrations in municipal wastewater, landfill leachate, leachate/drainage from mine tailings, car wash wastewater, and stormwater vary greatly (from 2 to >4 orders of magnitude). Flue gas condensate and textile factory concentrations, on the other hand, were less variable (one order of magnitude).

Precipitation, ion exchange, and sorption (or adsorption) are commonly applied technologies for metal removal. Precipitation is considered an inexpensive technique; its drawback is large sludge generation and less efficiency when metal concentrations are low. Ion exchange on the other hand, is highly efficient but considered more costly (Fu & Wang 2011; Carolin *et al.* 2017). Sorption technology is regarded as an attractive option for metal removal because it does not generate sludge and the operation is simple. Furthermore, it has the potential to be a low-cost technology (Sylwan & Thorin 2021). The application of pyrolysis to generate sorbents from waste materials has been investigated extensively (Xiang *et al.* 2020). One of the waste materials considered is sewage sludge, which could be dried and pyrolysed to produce sludge-derived char (Li *et al.* 2019; Huang *et al.* 2022).

Literature data indicated that non-activated and unmodified sludge-derived char had a maximum Cd sorption capacity in the range of 1.7–58 mg/g (Chen *et al.* 2014, 2015; Wongrod *et al.* 2018; Gao *et al.* 2019). Previous studies have investigated the Cd sorption capacity of sludge-derived char with respect to the influence of pyrolysis conditions (temperature and residence time), the addition of chemicals prior to or post pyrolysis (activation), and the embedding of various materials into the char structure (modification) (Chen *et al.* 2014; Tao *et al.* 2015; Sizmur *et al.* 2017). Increased pyrolysis temperature generates more developed microporosity, which means a larger area for sorption to occur. Furthermore, the ash content increased, which was linked to a larger cation exchange capacity and larger precipitation of metals (Chen *et al.* 2014; Gao *et al.* 2019). Typical temperature and time intervals investigated are in the range of 350–900 °C and 15–240 min, respectively (Chen *et al.* 2014, 2015; Wongrod *et al.* 2018; Gao *et al.* 2019).

While the importance of pyrolysis conditions has been highlighted, and various activation and modification procedures have been suggested, the different types of sludge generated during municipal wastewater treatment have not been considered. Previous studies were often conducted using artificial wastewaters (Rangabhashiyam *et al.* 2022) and did not consider the practical possibility to utilise the sludge-derived sorbent locally in real wastewater. Furthermore, while the cost of sludge-derived char production has been estimated in previous works (Barry *et al.* 2019; Cheng *et al.* 2020; Huang *et al.* 2022), the demand for sludge-derived char was not highlighted in these studies. Given these knowledge gaps, the purpose of this study is to investigate the Cd sorption capacity of char produced from primary sludge (PSC) compared with char produced from digested sludge (DSC). Primary sludge is generated from primary treatment of municipal wastewater. Digested sludge is a mixture of primary sludge and secondary sludge (from biological treatment) that has gone through anaerobic digestion to produce biogas. The characteristics of the two sludge types and chars produced are investigated to clarify the cause of the variation in sorption capacity. The feasibility of Cd sorbent generation from sludge was assessed based on sorption capacity in relation to the local demand for Cd sorbent. Furthermore, the pyrolysis energy balance was assessed to check the feasibility of sludge pyrolysis.

2. MATERIALS AND METHODS

2.1. Experimental

2.1.1. Collection, dewatering, and drying of sludge

Primary sludge and digested sludge (PS and DS) were collected at Käppala wastewater treatment plant (WWTP), Lidingö, Sweden, where wastewater is treated through grit removal, sand trap, primary settling, activated sludge process (pre-denitrification with simultaneous phosphorus precipitation and enhanced biological phosphorus removal), and sand filter polishing. Backwash water from sand filters is pumped back into the sand trap and thus influences the quality of PS. PS was collected directly following primary settling. DS was collected after dewatering, from a centrifuge. PS was manually dewatered in the laboratory using the following procedure: liquid polymer was added, and quick stirring was performed manually for 1 min, followed by slow stirring for 1 min. The mixture was left to stand for 1 h. The water was then successively decanted during a period of ~2 h. The amount of polymer added was 0.23 kg of liquid polymer per kg PS; the amount was determined based on

the total solids (TS) content of the sludge. The liquid polymer used was also collected from Käppala WWTP and contained 0.15% dry polymer (FLOPAM FO 4650 SSH, Chemifloc LTD). The drying of sludge was performed at 105 °C until the mass stabilised; for DS 24 h and for PS 30 h. The sludge was manually stirred every 2 h during the first 8 h of drying to prevent agglomeration.

2.1.2. Sludge characteristics

Characteristics of sludges as collected from the WWTP and after drying are shown in Table 1. Concentrations of metals (Hg, Pb, Cd, Cu, Cr, Ni Zn, Hg, and Ag) and moisture content were investigated. Furthermore, dried sludges were characterised with respect to ash content, elemental composition, calorific value, surface morphology, surface area (SSA), and pore size distribution. Metals in sludges as collected were determined by SGS Analytics, Linköping, Sweden. Metals in dried sludges were determined by ALS Scandinavia AB, Luleå, Sweden. Moisture content (SS-EN 12880-1:2000), ash content (SS28113), elemental composition (Thermo Scientific FlashSmart Elemental Analyzer, according to EN ISO 16948:2015), and calorific value (Parr 6200 Isoperibol Calorimeter, according to EN ISO 18125:2017) were determined in-house by Mälardalen University. The content of O was calculated by subtracting C, H, N, S, and ash from the total mass. The surface morphology was investigated through imaging in a field emission scanning electron microscope (FESEM; Carl Zeiss Microscopy GmbH, Jena, Germany). The FESEM was performed in-house at Oulu University, at an operating voltage of 5 kV. The SSA and pore size distribution were determined in-house by Oulu University according to the Brunauer–Emmett–Teller (BET) method, and the Non-local Density Functional Theory (NLDFT) based on a model of independent slit-shaped pores designed for carbonaceous materials. The measurement was performed using a sorptometer (3 Flex, Micromeritics Instrument Corp.,

Table 1 | Characterisation of primary sludge (PS) and digested sludge (DS; PS; and waste activated sludge), as collected from WWTP and in dried form

	Primary sludge (PS)		Digested sludge (DS)	
	As collected	Dried	As collected	Dried
Metal concentrations (mg/kg-TS)[a]				
Pb	4.8	5.3	16	12
Cd	0.27	0.25	0.73	0.60
Cu	160	152	420	404
Cr	6.1	9,8	19	28
Hg	0.11	0.13	0.45	0.34
Ni	6.1	6.4	21	19
Zn	220	204	510	443
Ag	0.68	–	1.8	–
Moisture (%)	95.7	5.1[b]	74.3	7.7[b]
Ash (% of DM)	–	9.4 ± 0.0	–	33.8 ± 0.0
Elemental composition (% of DM)				
C	–	46.2 ± 0.1	–	33.4 ± 0.03
H	–	6.64 ± 0.07	–	4.97 ± 0.03
N	–	3.0 ± 0.1	–	4.47 ± 0.01
S	–	0.53 ± 0.04	–	1.12 ± 0.04
O	–	34	–	22
Calorific value (MJ/kg DM)	–	21.0	–	15.1
SSA	–	0.70	–	1.00

Additional characterisation data with respect to dried sludge and its char is shown in Supplementary Material, Figure S1 (DM = dry mass; – = not determined).

[a]Mass balance calculation indicated that the mass of Cr in dried sludge, compared with sludge as collected, was ~160 and 140%, for PS and DS, respectively. Mass balance with respect to other metals was in the range 91–116% with respect to PS and 72–92% with respect to DS. This indicates that the concentrations in DS as collected may be underreported. Furthermore, there may be some contamination with Cr during sample handling.

[b]When fed into the pyrolysis reactor.

Norcross, GA, USA) according to the following procedure: each sample (100–200 mg) was degassed with Micromeritics smart VacPrep gas adsorption device at a pressure of 0.67 kPa and at a temperature of 413 K for 3 h to remove any previously adsorbed gas. The BET adsorption isotherms were obtained by the immersion of the sample tubes in liquid nitrogen (77.15 K) to achieve constant cryogenic temperature conditions and by dosing volumes of gaseous nitrogen in the samples.

2.1.3. Preparation of sludge-derived char

Prior to pyrolysis, the dried sludges were shredded and sieved to a particle size of <8 mm. Pyrolysis was performed in a tube furnace (Nabertherm, model R 120/500/12, equipped with a quartz glass tube, with a diameter of 120 mm, and length of 1,230 mm), under N_2 atmosphere. Sludge samples were placed in ceramic cups inside the furnace tube. The N_2 flow during oven heating and pyrolysis was 50 L/h, 1 bar. During cooling, a minimal N_2 flow was maintained, by reducing the pressure to 0.5 bar, to preserve the inert atmosphere in the oven. When the oven temperature during cooling reached 180 °C, the N_2 flow was stopped, and the outlet was sealed. Char was collected the following morning. After pyrolysis, the chars were ground and sieved (<0.250 mm). The pyrolysis heating rate was 20 °C/min. Three different residence time–temperature combinations were investigated: 400 °C–70 min; 800 °C–70 min; and 600 °C–120 min. Previous research showed that mineral components in sludge-derived char have a positive impact on the metal sorption capacity (Xu *et al.* 2017), and therefore chars were not washed prior to characterisation and sorption experiments.

2.1.4. Characterisation of sludge-derived char

Sludge-derived char was characterised prior to sorption experiments with respect to SSA, surface morphology, calorific value (higher heating value), elemental composition, and ash content (according to the same methods as were used for the characterisation of sludge, see Section 2.2). The metal content was analysed by ALS Life Sciences, Sweden. The pH of sludge-derived char was measured as follows: char was added to ultrapure water (solid to liquid, 1:10), the mixture was shaken for 5 min and then left to settle for 20 min, pH was then recorded in the liquid phase (using a Metrohm 744 pH meter). Investigation of surface functional groups was performed in a Thermo Fisher Nicolet iS50 FTIR Spectrometer, attenuated total reflection module, equipped with a germanium crystal. The pH at the point of zero charge (pH_{pzc}) was determined according to the procedure described by Messele *et al.* (2014). The pH of nine separate 0.01 M NaCl solutions was adjusted in the pH range of 5–13 using 0.1 M HCl or NaOH solution. Each pH-adjusted solution was then divided into three samples; two samples to which sorbent was added (2.5 g/L), and one blank sample. Samples and blanks were shaken at 300 rpm for 48 h, at room temperature. Finally, pH values were recorded (Mettler Toledo). The pH_{pzc} was determined by plotting the initial versus final pH of solutions and blanks, respectively, and identifying the intersection.

2.1.5. Cd sorption experiment

Cd solution was prepared from metal salt; cadmium nitrate, $Cd(NO_3)_2$. Ultrapure water was used to prepare a stock metal solution of pH 2 (1,000 mg/L) which was diluted to obtain the experiment's initial concentrations. Prior to the addition of sorbent, the initial pH of the metal solutions was adjusted to 5.0 ± 0.1, by the addition of acid/base (HNO_3/NaOH, 1 M). Initial pH 5 was chosen to avoid Cd removal through hydroxide precipitates (Zhai *et al.* 2004). Char (1 g/L) and metal solution (150 mg/L) were added to the sample container and subsequently shaken at 180 rpm using a reciprocating shaker. Following a contact time of 24 h, the sample pH was recorded, the samples were filtered (0.45 μm membrane filter), and the filtrate was collected for metal analysis. The experiment conditions were based on literature data (Supplementary Material, Figure S2 and Table S2). Initial concentration and char dosing were chosen at relevant levels to enable the identification of the maximum possible Cd sorption capacity. Blank samples, only ultrapure water, were prepared in an equivalent way. Samples for the determination of initial metal concentration were also adjusted to pH 5. A reference sample was kept at pH <2 and not filtered prior to analysis to confirm that no cadmium hydroxide precipitation and removal occurred during sample handling. All sorption experiments were performed at 18–25 °C. Cd concentrations in water were analysed by SGS Analytics, Linköping, Sweden.

Cd sorption (q_e, mg/g) was calculated as follows:

$$q_e = \frac{(C_0 - C_e) \times V}{m} \quad (1)$$

where C_0 (mg/L) is the initial concentration of metals, C_e (mg/L) is the final metal concentration (at equilibrium) after separation of the sorbent, V (L) is the volume of the sample, and m (g) is the mass of sorbent (sludge-derived char) (char dose: $(m/V) = D$). Under the given experimental conditions and based on the aforementioned literature data q_e was assumed to be close to the maximum sorption capacity (Q_{max}).

2.2 Energy balance calculations

To investigate the energy balance of pyrolysis, the pyrolysis vapours were assumed to be combusted to support the pyrolysis process. All calculations were made with respect to kg of dewatered sludge feedstock (primary or digested sludge), and assuming solids content of dewatered primary/digested sludge (DM_{dew}, %) of 25% (Table 1; Kim & Parker 2008). The energy balance of pyrolysis (E_{net}, kJ/kg dewatered sludge), i.e., net output in the form of heat or non-combusted pyrolysis vapours, was calculated as:

$$E_{net} = E_{vap} \times 0.85 - (E_{drying} + E_{heating} + E_{pyro}) \quad (2)$$

where E_{vap} is the energy content in pyrolysis vapours, E_{drying} is the energy requirements for drying dewatered sludge, $E_{heating}$ is the energy required for heating the dried sludge to pyrolysis temperature, and E_{pyro} is the energy required for the pyrolysis reaction. Radiative heat losses and incomplete combustion will limit the utilisation of energy from pyrolysis vapours; thus E_{vap} was multiplied by 0.85 (Wang *et al.* 2012; Marazza *et al.* 2019). The energy in pyrolysis vapours (E_{vap}) was assumed to equal the difference in energy between feedstock sludge and the char:

$$E_{vap} = (E_{dry\ sludge} - E_{char} \times Y_{char}) \times (DM_{dew}) \quad (3)$$

where $E_{dry\ sludge}$ (kJ/kg) is the calorific value of dried sludge (Table 1), and E_{char} (kJ/kg) is the calorific value of char. The latter was multiplied by the char yield (Y_{char}, %) to find the energy per kg of dried sludge input. To calculate the amount of energy in relation to kg of dewatered sludge feedstock, multiplication was made by the solids content of dewatered sludge (DM_{dew}, %). E_{drying} and $E_{heating}$ were calculated as follows:

$$E_{drying} = (\Delta H_{vap} + C_{p,water} \times \Delta T_{100}) \times (1 - DM_{dew}) \quad (4)$$

$$E_{heating} = C_{p,sludge} \times \Delta T_{pyro} \times DM_{dew} \quad (5)$$

where ΔH_{vap} (kJ/kg) is the enthalpy of vaporisation of water, $C_{p,water}$ (kJ/kg, °C) is the specific heat capacity of water, ΔT_{100} (°C) is the difference between initial temperature (20 °C) and 105 °C, $C_{p,sludge}$ (kJ/kg, °C) is the specific heat capacity of dried sludge, and ΔT_{pyro} (°C) is the difference between the initial temperature (105 °C) and the pyrolysis temperature. The energy required for heating of sludge solids was not considered in the calculation of E_{drying}, because it was assumed to be minor compared to the energy required to heat intrinsic water (Kim & Parker 2008). The energy for the pyrolysis reaction (E_{pyro}) was approximated to 38 kJ/kg of dewatered sludge (based on 150 kJ/kg dried sludge (Wang *et al.* 2012) and DM_{dew}). The heat losses associated with extended pyrolysis residence time were not considered. The following parameter values were assumed: ΔH_{vap}, 2,090 kJ/kg; $C_{p,water}$, 4.18 kJ/kg, °C; and $C_{p,sludge}$, 1.95 kJ/kg, °C (Kim & Parker 2008).

In a WWTP where anaerobic digestion is implemented, the pyrolysis of undigested PS would decrease the biogas yield significantly. The unexploited energy in methane (E_{CH4}) was thus subtracted from E_{net} in the case of primary sludge pyrolysis. E_{CH4} (kJ/kg dewatered sludge) was estimated as follows:

$$E_{CH4} = VS \times LHV_{CH4} \times V_{CH4} \times DM_{dew} = 0.906 \times 35{,}880 \times 0.33 \times 0.25 = 2{,}680 \quad (6)$$

where VS is the content of volatile solids in PS (kg VS/kg DM; based on ash content according to Table 1), E_{CH4} is the lower heating value of methane (35,880 kJ/Nm^3; Ruffino *et al.* 2020), and V_{CH4} is the methane production, which was estimated to 0.33 Nm^3/kg VS based on the literature data (Ruffino *et al.* 2015, 2020).

2.3. Local sorbent demand

The local demand for Cd sorbent was assessed based on literature data and personal communication with stakeholders. Västerås city, Sweden, was chosen as the study location. The assessment considered municipal wastewater and stormwater

generated in the city as well as industrial effluents generated within a travelling distance of 2 h. Cd concentrations and volumetric flows were documented and based on this data the total mass of Cd (kg/year) was estimated.

The local sorbent demand was compared with the Cd sorption capacity of the char generated from pyrolysis of sludge produced at Kungsängsverket WWTP in Västerås. To indicate the mass of Cd which could be sorbed yearly ($M_{Cd,yr}$, kg/year), the char sorption capacity (q_e, kg/tonne) was multiplied by the char yield (Y, %) and yearly sludge production ($M_{\text{sludge.year}}$, tonne/year):

$$M_{\text{Cd,year}} = q_e \times Y \times M_{\text{sludge.year}} \tag{7}$$

The value of q_e, at relevant sorbate concentration, was estimated based on literature data and the linear form of the Langmuir isotherm model (Langmuir 1918), which is valid when sorbate concentrations are low (Tran *et al.* 2017):

$$q_e = Q_{\max} K_L C_e \tag{8}$$

where K_L is the Langmuir constant, representing the affinity between sorbent and sorbate. The required dosing of sorbent (D, g/L) was estimated as (combining Equation (1) and (8)):

$$D = \frac{(C_O - C_e)}{Q_{\max} K_l C_e} \tag{9}$$

3. RESULTS AND DISCUSSION

3.1. Characteristics of sludge-derived char and its influence on Cd sorption capacity

The char yield, sorption capacity, SSA (BET isotherm plots are shown in Supplementary Material, Figure S3), pore structure, calorific value, elemental composition, ash content, pH, and pH_{pzc} are given in Table 2 (correlations are illustrated in Supplementary Material, Figures S4–S6). The char yield for the respective sludges decreased with increasing pyrolysis temperature (and increased carbonisation), while char ash content, pH, and pH_{pzc} increased. Similar trends were reported by Chen *et al.* (2014). The increasing pH and pH_{pzc} is a result of the increased fraction of ash mineral components and the release of alkali salts from the organic matrix. The yields and ash contents were higher for DS compared with PS, which is explained by the higher original ash content in DS.

The SSA increased with a higher pyrolysis temperature. The most pronounced increase occurred between 600 and 800 °C. Successively longer carbon chains are degraded as pyrolysis temperature increases (Chen *et al.* 2014). This is generally beneficial for the development of pore structure and SSA. However, pore enlargement due to volatile losses in the range 550–650 °C may limit the SSA development (Xu *et al.* 2017). Notably, the SSA was highly correlated with the fraction of micropores in char (correlation coefficient 0.90). However, while micropore fraction increased in $PSC_{600\text{-}120}$ compared with $PSC_{400\text{-}70}$, the SSA did not increase significantly.

FESEM images (Figure 1 and Supplementary Material, Figures S7–S8) show that that the surface morphologies of PSCs and DSCs are different. The PSC samples (Figures 1(b) and 1(c)) include mainly long carbon chains while DSC (Figures 1(e) and 1(f)) has a rough surface with voids and cracks. The PSCs and DSCs are more porous compared with raw materials PS and DS (Figures 1(a) and 1(d), respectively), and porosity is larger at higher pyrolysis temperature. This observation is in line with the increasing SSA at higher pyrolysis temperature. The surface morphology after sorption of Cd was not investigated herein; however, previous works found an increased surface roughness and formation of granular crystals after sorption of Cd (Chen *et al.* 2015; Gao *et al.* 2019).

The calorific value of PSC was close to that of dried PS. With respect to DSC, the calorific value decreased with increasing pyrolysis temperature, in proportion to the decreasing yield (Supplementary Material, Figure S4). The energy contents of dried sludges and chars were comparable to those found in previous studies (dried PS: 23 MJ/kg DM; PSC: 17–21 MJ/kg DM; DS: 17 MJ/kg DM; DSC: 10–16 MJ/kg DM) (Kim & Parker 2008).

With respect to elemental composition, O, H, and N content decreased with a higher pyrolysis temperature, while S content increased (Table 2). The C content increased slightly with increasing pyrolysis temperature in PSC while it decreased slightly in DSC. Increase of C content in PSC may be linked to the carbonisation process. DSC has been previously

Table 2 | Char characteristics

Char	Yield (%)	$q_{e,cd}$ (mg/g)	SSA (m^2/g)	Micro/meso/ macropores (%)[a]	Total pore vol. (cm^3/g)[b]	Calorific value (MJ/kg DM)	Elemental composition (%)					Ash (% of dry matter)	pH	pH_{pzc}
							C	H	N	S	O			
$PSC_{400\text{-}70}$	31.5	4.9(0.7)	4.56	11/77/12	0.012	21.1(< 0.1)	51.6(0.3)	2.97(0.04)	4.74(0.04)	0.34(0.00)	11.0	29.3(0.0)	8.56	7.7
$PSC_{600\text{-}120}$	26.8	1.8(2.3)	4.59	13/78/9	0.010	20.9(< 0.1)	55.1(0.0)	1.40(0.02)	3.93(0.02)	0.42(0.00)	4.7	34.4(0.3)	10.77	11.0
$PSC_{800\text{-}70}$	23.9	9.0(0.1)	30.24	17/78/5	0.047	20.0(0.1)	55.3(0.1)	0.75(0.05)	1.89(0.01)	0.58(0.01)	2.7	38.8(0.2)	11.33	11.0
$DSC_{400\text{-}70}$	58.4	1.7(−)[c]	9.86	7/81/12	0.032	12.6(< 0.1)	30.7(0.1)	2.32(0.02)	3.80(0.01)	0.71(0.01)	4.4	58.0(0.7)	8.15	7.5
$DSC_{600\text{-}120}$	48.0	0.9(1.2)	15.04	10/84/6	0.035	10.2(0.1)	27.9(0.5)	0.75(0.02)	2.63(0.02)	0.92(0.02)	0[d]	69.3(0.3)	10.64	8.6
$DSC_{800\text{-}70}$	44.4	6.1(1.2)	87.13	25/70/5	0.10	9.2(< 0.1)	26.2(0.2)	0.31(0.00)	0.99(0.01)	1.04(1.04)	0[d]	73.8(0.2)	10.39	7.9

Standard deviation of duplicate samples is given in parenthesis. DM, dry mass; SSA, specific surface area.

[a]Micro-, meso-, and macro-pores defined as <2, 2–50, and >50 nm, respectively.

[b]For pore widths >0.7 nm.

[c]Only one replicate. One datapoint was removed due to outlying result (concentration after sorption experiment higher than concentration before experiment).

[d]Calculation resulted in slightly negative values (–2.4 and −1.5%, respectively), which may be due to inhomogeneity in the samples.

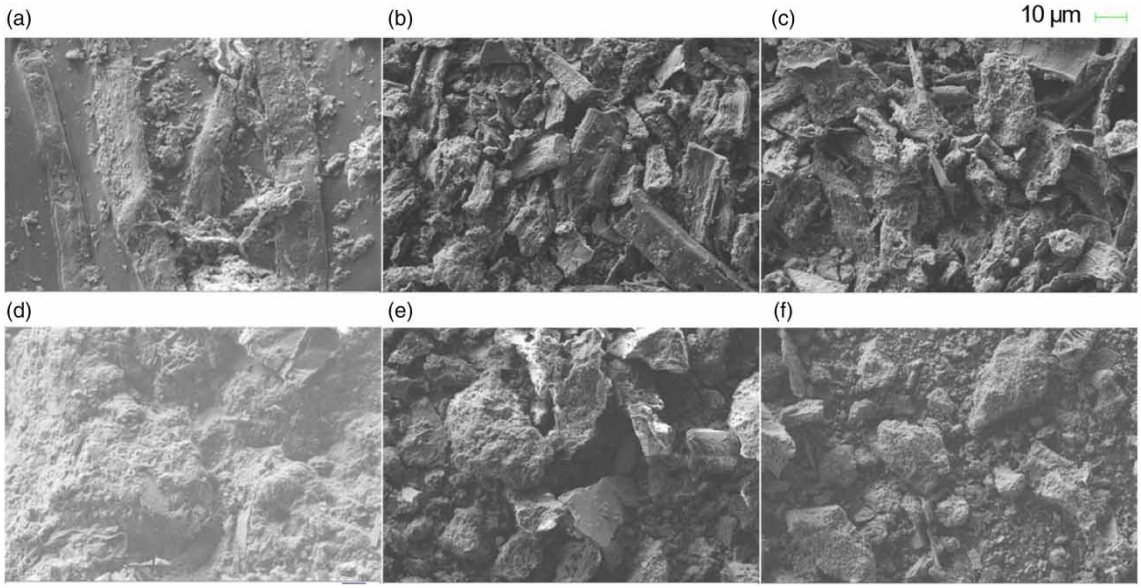

Figure 1 | FESEM images of dried sludges and chars prior to sorption experiment: (a) PS; (b) $PSC_{400\text{-}70}$; (c) $PSC_{800\text{-}70}$; (d) DS; (e) $DSC_{400\text{-}70}$; and (f) $PSC_{800\text{-}70}$.

biologically degraded during anaerobic digestion and contains a lower amount of easily degradable components when the pyrolysis process is initiated. The enrichment of carbon during pyrolysis (carbon content in char in relation to the carbon content of the pyrolysis substrate) was previously shown to be larger for sludges that were less degraded (and had a larger fulvic acid content) (Méndez *et al.* 2005).

The metal contents in dried sludge and chars, at pyrolysis temperature 400 and 800 °C, are shown in Figure 2. Cd and Hg were volatilised during pyrolysis; Hg from 400 °C, and Cd at 800 °C, where concentrations in char were below the

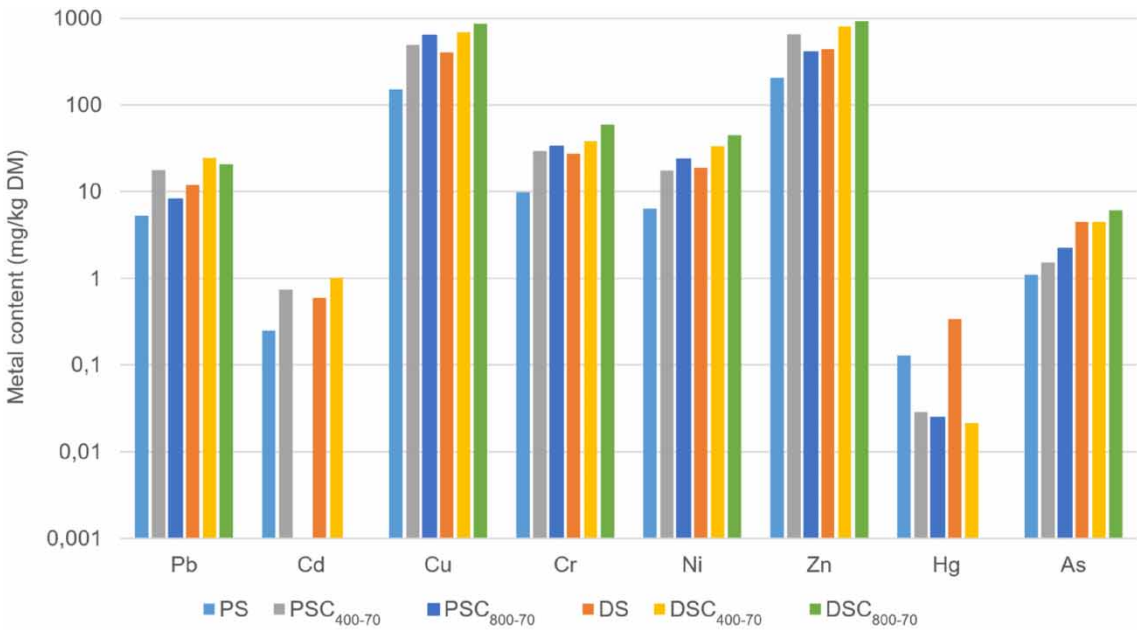

Figure 2 | Metal contents in chars generated at pyrolysis temperature 400 and 800 °C, and corresponding data for dried sludges (also given in Table 1). Concentrations of Cd in $PSC_{800\text{-}70}$ and $DSC_{800\text{-}70}$, and Hg in $DSC_{800\text{-}70}$ were below the detection limit (0.02 mg/kg dry mass).

concentrations in dried sludge substrate. All the other metals investigated increased in concentration when comparing char with dried sludge substrate.

Fourier transform infrared (FTIR) analysis (spectra shown in Supplementary Material, Figure S9) confirmed the decomposition and aromatisation that occurred during pyrolysis. Dried PS contained O–H bonds, found in alcohols or carboxylic acids (broad band around 3,350) (Hossain *et al.* 2011; Kim *et al.* 2012; Lu *et al.* 2012). FTIR spectra indicated that these bonds decomposed during pyrolysis. No O–H peak was seen for DS, which may be due to the (previous) decomposition of sludge that occurred during digestion. The aromatisation or organic matter decomposition was also indicated by the destruction of C–H bonds in both PS and DS (the disappearance of narrow weak bands at ~2,920 and ~2,855 cm^{-1}) (Zhang *et al.* 2013). The bands at ~1,600 cm^{-1} may indicate stretching of aliphatic or aromatic C=C and C=O bonds (Kim *et al.* 2012; Lu *et al.* 2012). These peaks could slightly shift or decrease due to increased aromaticity, which was seen as the pyrolysis temperature increased. In the fingerprint region (<1,450 cm^{-1}), carbon–carbon (C–C) and carbon–oxygen (C–O) bonds absorb infrared (IR) at a wide range of wavenumbers (Clark 2020) and may contribute to a combined peak at ~1,000 cm^{-1}. Comparing the FTIR spectra of PS, DS, and the respective chars, it appears that PS as a starting material has a richer functional group composition compared with DS, which is in line with the observed sorption capacities and oxygen content of the chars. The surface functional groups could thus contribute to balancing the lacking SSA of PSC compared with DSC.

Cd sorption capacity for the respective char type (PSC and DSC; Figure 3) increased with a more developed pore structure (Figure 1), larger SSA and higher pyrolysis temperature. PSC had a larger Cd sorption capacity than DSC irrespective of pyrolysis temperature, though its SSA was smaller. The maximum Cd sorption capacity found was 9.0 mg/g (for $PSC_{800\text{-}70}$). The sorption capacity is of similar magnitude as the literature data with respect to unmodified sludge-derived char; 1.7 mg/g to 58 mg/g (Chen *et al.* 2014; Wongrod *et al.* 2018; Gao *et al.*, 2019). The following characteristics of PSC may compensate for the lacking SSA:

- Cationic elements were accumulated in PSC (comparable or larger Ca, K, and Na contents compared with those in DSC; Supplementary Material, Figure S1), which indicates that cation exchange was one of the Cd sorption mechanisms involved (Chen *et al.* 2014).
- PSC had a higher pH compared with the DSCs, which indicates that precipitation of Cd also contributed to the higher Cd sorption capacity.
- The lack of functional groups, in both chars (based on FTIR analysis), indicates that complexation is not a dominant sorption mechanism. However, the results indicated that PS had a richer functional group composition compared with DS; the O–H and C=O bonds in PS indicate the presence of carboxylic groups which could form complexes with Cd. The potential

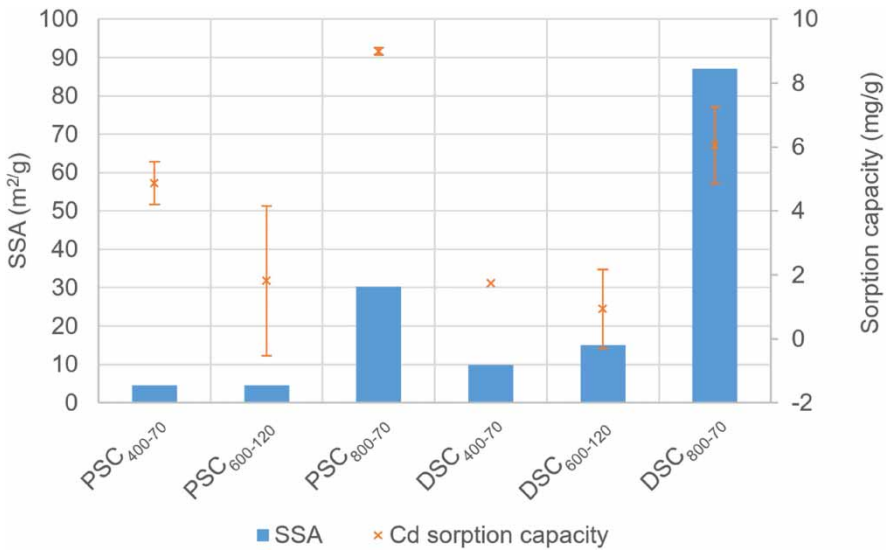

Figure 3 | Sorption capacity and SSA of DSC and PSC (one replicate with respect to Cd sorption onto $DSC_{400\text{-}70}$). Final pH in solution 5.26–5.84, which is below the value for formation of Cd hydroxide precipitates (pH 8.3; Özer and Tümen 2003).

presence of carboxylic groups is also supported by the larger concentration of O in the PSCs compared with DSCs. Thus, though complexation may be a minor mechanism, the results point to a larger complexation capacity of PSC compared with DSC. Furthermore, greater N content in PSCs compared to DSCs may indicate more amino groups which may be involved in the complexation of Cd (Morshedy *et al.* 2021).

- The PSCs had a higher pH_{pzc} compared with the DSC, indicating a more positive surface charge (Messele *et al.* 2014). This indicated that electrostatic attraction was not a dominant sorption mechanism. The higher pH_{pzc} may be explained by the previously mentioned accumulation of cations.

3.2. Energy balance of pyrolysis

Experimental data and calculations indicate that energy in pyrolysis vapours is sufficient to support the sludge pyrolysis (Figure 4). With increased pyrolysis temperature, the energy balance shifts so that the surplus energy increases, mainly due to the increased generation of pyrolysis vapours, which is larger than the increase of energy required for heating the pyrolysis process. PS pyrolysis has a more positive energy balance compared with DS pyrolysis, due to larger initial calorific value (~39%). Similar results were found by Kim & Parker (2008), who found PS to have 35% larger energy content than DS, per kg dry sludge. However, given the assumed loss of biogas production (when PS is not digested) the energy balance of PS pyrolysis is negative. Buonocore *et al.* (2015) found a similar energy use for the drying of sludge (~2,000 kJ/kg dewatered sludge or 937 MJ/472 kg dry sludge, dewatered from 75 to 10% moisture content). Uncertainty exists with respect to the net excess energy because energy required to maintain the temperature during residence time was not considered. A previous study based on modelling indicated that, due to energy losses, the energy in pyrolysis vapours (syngas and oil) covered ~80% of the energy needed for drying (from 73 to 10% moisture) and pyrolysis of digested sludge at 500 °C (Salman *et al.* 2019).

3.3. Cd sorbent production in relation to local need for sorbent

3.3.1. Local demand for Cd sorbent

One of the main Cd loads to the local WWTP is household wastewater, contributing with ~1.4 kg/year and representing ~64% of the total load (Renström 2018). The largest point source of Cd to the municipal wastewater system was identified as leachate from the local waste management site, contributing ~0.05 kg/year (ibid.). The Cd concentration and load in leachate prior to wastewater treatment were therefore investigated. Additionally, substantial amounts of Cd were identified in

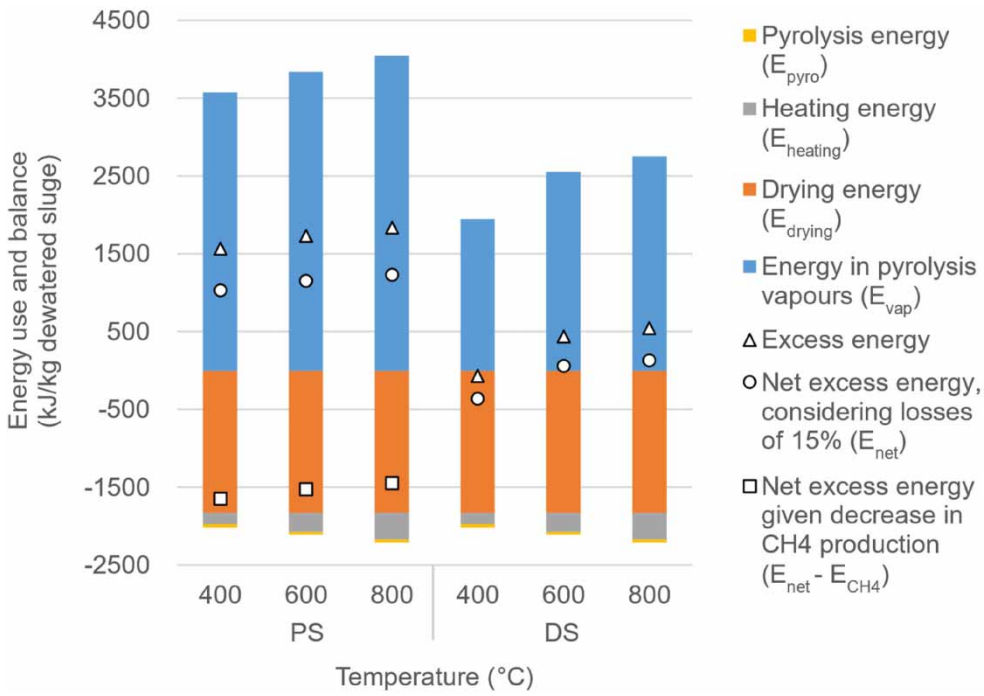

Figure 4 | Energy use and balance with respect to PS and DS pyrolysis (based on Equations (2)–(6)).

flue gas condensate at a local combined heat and power (CHP) plant (Eskilstuna, distance 45 km), in water from local mines (Garpenberg, 96 km; and Lovisagruvan, 111 km; and Zinkgruvan, 157 km). A local tannery (Tärnsjö Garveri, distance 81 km) was identified; however, they apply vegetable-based tanning, and the Cd concentration is therefore insignificant (not regularly measured; Torgny Eriksson, personal communication, 1 June 2023). Furthermore, stormwater may contain significant amounts of Cd (Renström 2018). The estimated yearly amounts of Cd in the identified wastewaters are summarised in Table 3.

It was found that car wash wastewater could be one of the main sources of Cd locally (Sörme & Lagerkvist 2002); however, it was estimated to contribute only ~1% of Cd locally (Renström 2018) and was therefore not included in the analysis. Around 7% of the Cd load to the local WWTP was estimated to come from water seeping from the ground into wastewater pipes (ibid.). This water is not easily treated and has thus not been included in Table 3. Another major contribution to municipal wastewater, in a number of Swedish cities, was identified as artist paints (Levlin *et al.* 2001), which in one study approximated to ~10% (Sörme & Lagerkvist 2002). This source is not easily controlled by wastewater treatment but rather by the user's knowledge on how to handle the paint to avoid contamination. Another major Cd contribution (7% of load to WWTP) was identified as wastewater from the manual cleaning of floors at car service stations (Renström 2018); however, recommendations are that such wastewater should not be released without prior treatment.

In freshwaters, Cd is regulated under what is known as environmental quality standards (EQS) which allow for an annual average concentration of 0.08–0.25 μg Cd/L (depending on water hardness) (European Commission 2008).

3.3.2. Cd sorption capacity of locally produced char

To reach maximum Cd sorption capacity (experimentally determined Q_{max}: 6.1 mg/g, DSC), the sorbate concentration needs to be at least ~100 mg/L (Chen *et al.* 2014; Wongrod *et al.* 2018). Given that Q_{max} could be achieved (from highly contaminated wastewater) the sorption capacity of DSC is 7,900 kg/year ($Y = 44.4\%$, $M_{sludge.yr} = 2{,}935$ tonne/year). With respect to PSC, though the sorption capacity per mg was higher, a similar accumulated sorption capacity was calculated due to the smaller PSC yield; 8,100 kg/year ($Y = 23.9\%$, $M_{sludge.yr} = 3{,}750$ tonne/year). Given the concentrations in local wastewater (Table 3; sorbate concentration ~1 μg/L or less), the q_e value was calculated based on literature data and sorption isotherms (Table 4). The approximate Cd sorption capacity of DSC based on q_e values according to Table 4 is 3–71 kg/year, which indicates that it could be possible to cover the local demand for Cd sorbent (Table 3) by using DSC or PSC. Based on isotherm model parameters according to Chen *et al.* (2021), the required dosing of char to reach 50 and 90% removal of Cd at initial

Table 3 | Local Cd bearing wastewater in or in the vicinity of Västerås city, and the associated yearly masses of Cd (n.a. = data not available)

Activity	Cd concentration (μg/L)	Wastewater flow (m^3/year)	Amount of Cd (kg/year)	Reference
Incoming load to municipal wastewater treatment plant, Kungsängsverket, Västerås	0.06–0.16[a]	17,885,525	2.4[b]	Mälarenergi (2022)
Waste site, Gryta, Västerås[c]	~0.26	~170,000	~0.05	Linus Fogelberg, personal communication, March 2023
CHP plant, Eskilstuna	0.5	150,000	0.08	Jesper Lymar, personal communication, April 2022.
Mining wastewater, Garpenberg	0.4	3,000,000	1.2	Adolfsson *et al.* (2020)
Mining wastewater, Lovisagruvan	9.1	44,000	0.4	Sartz & Bäckström (2013)
Mining wastewater, Zinkgruvan	25 (mine water); 10 (process water)	n.a.	n.a.	Andersson (2003)
Stormwater	0.14–0.99	18,700,000	9	(Gustav Myhrman, personal communication, Aug 2023)[d]
Total			13	

[a]Influent Cd is not monitored regularly. Value based on 33 historical measurements during 2017–2019, after four outlier values were excluded. Average concentration: 0.13 μg/L.
[b]Summary of the amounts in effluent water and sludge.
[c]Data for 2021. This load goes to the municipal wastewater treatment plant (after treatment on site). Additionally, ~0.02 kg/year is released to local recipient. Ion exchange resins are used upstream of this point to treat smaller flows (~700 m^3/year) with larger Cd concentration (~25 μg/L) (Linus Fogelberg, personal communication, June 2023). The current treatment does not target Cd specifically.
[d]Based on modelling.

Table 4 | Cd sorption capacity (q_e) at sorbate concentration 1 μg/L (n.d. = not determined)

Q_{max} (mg/g)	q_e(mg/g)	Reference	Char amendment, modification, or activation
115	0.05	Chen *et al.* (2021)	Hydroxyapatite modification
n.d.	0.02	Sylwan & Thorin (2023)	No
62	0.002	Ni *et al.* (2019)	No

concentration 1 μg/L is 20 and 170 mg/L, respectively. This can be compared to the currently used ion exchange resin at Eskilstuna CHP, for which the estimated consumption was ~3 mg/L (Jesper Lymar, personal communication, April 2022).

4. CONCLUSIONS

This study investigated selected feasibility aspects of producing a Cd sorbent from primary and digested sludges. Experimental results showed that the sorption capacity of PSC (9.1 mg Cd/g; 800 °C, 70 min) was larger than that of DSC (6.0 mg Cd/g; 800 °C, 70 min), even though PSC had a less developed surface structure and smaller SSA compared with DSC. Characterisation of the respective chars indicated that sorption onto PSC was favoured by larger ion exchange capacity, precipitation, and complexation capacity. Assessment of the total Cd sorption capacity of char produced from a local WWTP indicated that PSC could sorb larger amounts of Cd compared with DSC (8,100 and 7,900 kg/year, respectively; PSC yield is smaller compared with DSC yield). These findings underscore the feasibility of repurposing waste carbon-based materials for precise, localised industrial applications. Further research is suggested to implement similar approaches to mitigate the environmental impact of other toxic metal compounds. The assessment of local Cd bearing wastewater indicated that sludge-derived char could cover the need for Cd sorbent locally (13 kg/year), though the Cd sorption capacity of char (3–71 kg/year) will be far below the maximum capacity at Cd concentrations relevant to the identified wastewaters. However, the volumes of char required to achieve similar Cd removal as in current systems may be large compared with the current substrates used, which will lessen the feasibility. The energy balance of sludge pyrolysis was theoretically assessed based on the calorific values of sludges, indicating that energy contained in pyrolysis vapours could support the drying and pyrolysis of digested sludge. Further investigations are recommended to explore the sorption capacity of sludge-derived char at metal concentrations relevant to real wastewater and also to investigate the energy balance of full-scale sludge pyrolysis.

ACKNOWLEDGEMENTS

The authors would like to thank Anna Bogren, Agnieszka Juszkiewicz, and Anna Lindgren for input data with respect to the experimental plans and objectives. Thanks to Robert Tryzell, Joakim Jansson, Sebastian Schwede, and Ryan Merckel for assistance in setting up the pyrolysis equipment. Thanks to Jesper Olsson for assistance in collecting sludge samples, and to Ali Ahmad Shahnawazi and Palle Hedlund for assistance during sludge pyrolysis. Thanks to Riikka Koski for contributing to physisorption measurements, to Tao Hu for FESEM analysis, and to Mikko Häkkinen for his contribution in pH_{pzc} measurements.

DATA AVAILABILITY STATEMENT

All relevant data are included in the paper or its Supplementary Information.

CONFLICT OF INTEREST

The authors declare there is no conflict.

REFERENCES

Adolfsson, A., Edström, J., Hedin, K., Tanse, L., Bolin, N.-J. & Suup, M. 2020 Teknisk beskrivning av Bolidens gruvverksamhet i Garpenberg vid en utökad årlig produktion till 3,5 miljoner ton malm [WWW Document]. Available from: https://www.boliden.com/globalassets/operations/mines/garpenberg/dokument-2020/slutversion-teknisk-beskrivning-andringstillstand-garpenberg-200930.pdf (accessed 26 May 2023).

Andersson, K. 2003 Gruvvattenrening med hjälp av anrikningssand [WWW Document]. Available from: https://www.diva-portal.org/smash/get/diva2:881008/FULLTEXT01.pdf (accessed 31 May 2023).

Arti, R. & Mehra, R. 2023 Analysis of heavy metals and toxicity level in the tannery effluent and the environs. *Environ Monit Assess* **195**. https://doi.org/10.1007/s10661-023-11154-4.

Barry, D., Barbiero, C., Briens, C. & Berruti, F. 2019 Pyrolysis as an economical and ecological treatment option for municipal sewage sludge. *Biomass Bioenergy* **122**, 472–480. https://doi.org/10.1016/j.biombioe.2019.01.041.

Bogush, A. A. & Voronin, V. G. 2011 Application of a peat-humic agent for treatment of acid mine drainage. *Mine Water Environ* **30**, 185–190. https://doi.org/10.1007/s10230-010-0132-2.

Buonocore, E., Mellino, S., De Angelis, G., Liu, G. & Ulgiati, S. 2015 Life cycle assessment indicators of urban wastewater and sewage sludge treatment. *Ecol Indic* **94**, 13–23. https://doi.org/10.1016/j.ecolind.2016.04.047.

Carolin, C. F., Kumar, P. S., Saravanan, A., Joshiba, G. J. & Naushad, M. 2017 Efficient techniques for the removal of toxic heavy metals from aquatic environment: a review. *J Environ Chem Eng* **5**, 2782–2799. https://doi.org/10.1016/j.jece.2017.05.029.

Chen, T., Zhang, Y., Wang, H., Lu, W., Zhou, Z., Zhang, Y. & Ren, L. 2014 Influence of pyrolysis temperature on characteristics and heavy metal adsorptive performance of biochar derived from municipal sewage sludge. *Bioresour Technol* **164**, 47–54. https://doi.org/10.1016/j.biortech.2014.04.048.

Chen, T., Zhou, Z., Han, R., Meng, R., Wang, H. & Lu, W. 2015 Adsorption of cadmium by biochar derived from municipal sewage sludge: impact factors and adsorption mechanism. *Chemosphere* **134**, 286–293. https://doi.org/10.1016/j.chemosphere.2015.04.052.

Chen, Y., Li, M., Li, Y., Liu, Y., Chen, Y., Li, H., Li, L., Xu, F., Jiang, H. & Chen, L. 2021 Hydroxyapatite modified sludge-based biochar for the adsorption of Cu^{2+} and Cd^{2+}: adsorption behavior and mechanisms. *Bioresour Technol* **321**. https://doi.org/10.1016/j.biortech.2020.124413.

Cheng, F., Luo, H. & Colosi, L. M. 2020 Slow pyrolysis as a platform for negative emissions technology: an integration of machine learning models, life cycle assessment, and economic analysis. *Energy Convers Manage* **223**. https://doi.org/10.1016/j.enconman.2020.113258.

Choubert, J. M., Pomiès, M., Martin Ruel, S. & Coquery, M. 2011 Influent concentrations and removal performances of metals through municipal wastewater treatment processes. *Water Sci Technol* **63**, 1967–1973. https://doi.org/10.2166/wst.2011.126.

Clark, J. 2020 Identifying the Presence of Particular Groups [WWW Document]. Available from: https://chem.libretexts.org/@go/page/3734 (accessed 16 November 2021).

European Commission 2008 Directive 2008/105/EC of the European parliament and of the council of 16 December 2008 on environmental quality standards in the field of water policy. *Off J L* **348**, 84–97.

Fu, F. & Wang, Q. 2011 Removal of heavy metal ions from wastewaters: a review. *J Environ Manage* **92**, 407–418. https://doi.org/10.1016/j.jenvman.2010.11.011.

Gao, L. Y., Deng, J. H., Huang, G. F., Li, K., Cai, K. Z., Liu, Y. & Huang, F. 2019 Relative distribution of Cd^{2+} adsorption mechanisms on biochars derived from rice straw and sewage sludge. *Bioresour Technol* **272**, 114–122. https://doi.org/10.1016/j.biortech.2018.09.138.

Göbel, P., Dierkes, C. & Coldewey, W. G. 2007 Storm water runoff concentration matrix for urban areas. *J Contam Hydrol* **91**, 26–42. https://doi.org/10.1016/j.jconhyd.2006.08.008.

Hossain, M. K., Strezov Vladimir, V., Chan, K. Y., Ziolkowski, A. & Nelson, P. F. 2011 Influence of pyrolysis temperature on production and nutrient properties of wastewater sludge biochar. *J Environ Manage* **92**, 223–228. https://doi.org/10.1016/j.jenvman.2010.09.008.

Huang, L., Rad, S., Xu, L., Gui, L., Song, X., Li, Y., Wu, Z. & Chen, Z. 2020 Heavy metals distribution, sources, and ecological risk assessment in Huixian wetland, south China. *Water (Basel)* **12**. https://doi.org/10.3390/w12020431.

Huang, C., Mohamed, B. A. & Li, L. Y. 2022 Comparative life-cycle assessment of pyrolysis processes for producing bio-oil, biochar, and activated carbon from sewage sludge. *Resour Conserv Recycl* **181**. https://doi.org/10.1016/j.resconrec.2022.106273.

Kim, Y. & Parker, W. 2008 A technical and economic evaluation of the pyrolysis of sewage sludge for the production of bio-oil. *Bioresour Technol* **99**, 1409–1416. https://doi.org/10.1016/j.biortech.2007.01.056.

Kim, K. H., Kim, J. Y., Cho, T. S. & Choi, J. W. 2012 Influence of pyrolysis temperature on physicochemical properties of biochar obtained from the fast pyrolysis of pitch pine (*Pinus rigida*). *Bioresour Technol* **118**, 158–162. https://doi.org/10.1016/j.biortech.2012.04.094.

Langmuir, I. 1918 The adsorption of gases on plane surfaces of glass, mica and platinum. *J Am Chem Soc* **40**, 1361–1403.

Levlin, E., Tideström, H., Kapilashrami, S., Stark, K. & Hultman, B. 2001 *Slamkvalitet och trender för slamhantering*. VA-Forsk Rapport 2001-05. Stockholm.

Li, S., Yao, Y., Zhao, T., Wang, M. & Wu, F. 2019 Biochars preparation from waste sludge and composts under different carbonization conditions and their Pb(II) adsorption behaviors. *Water Sci Technol* **80**, 1063–1075. https://doi.org/10.2166/wst.2019.353.

Lu, H., Zhang, W., Yang, Y., Huang, X., Wang, S. & Qiu, R. 2012 Relative distribution of Pb^{2+} sorption mechanisms by sludge-derived biochar. *Water Res* **46**, 854–862. https://doi.org/10.1016/j.watres.2011.11.058.

Mälarenergi 2022 Miljörapport Kungsängens reningsverk 2021 [WWW Document]. Available from: https://www.malarenergi.se/globalassets/dokument/miljorapporter/miljorapport-kungsangens-2021.pdf (accessed 17 April 2023).

Marazza, D., Macrelli, S., D'Angeli, M., Righi, S., Hornung, A. & Contin, A. 2019 Greenhouse gas savings and energy balance of sewage sludge treated through an enhanced intermediate pyrolysis screw reactor combined with a reforming process. *Waste Manage* **91**, 42–53. https://doi.org/10.1016/j.wasman.2019.04.054.

Méndez, A., Gascó, G., Freitas, M. M. A., Siebielec, G., Stuczynski, T. & Figueiredo, J. L. 2005 Preparation of carbon-based adsorbents from pyrolysis and air activation of sewage sludges. *Chem Eng J* **108**, 169–177. https://doi.org/10.1016/j.cej.2005.01.015.

Messele, S. A., Soares, O. S. G. P., Órfão, J. J. M., Stüber, F., Bengoa, C., Fortuny, A., Fabregat, A. & Font, J. 2014 Zero-valent iron supported on nitrogen-containing activated carbon for catalytic wet peroxide oxidation of phenol. *Appl Catal B* **154–155**, 329–338. https://doi.org/10.1016/j.apcatb.2014.02.033.

Morshedy, A. S., Galhoum, A. A., Aleem, A. A. H. A., Shehab El-din, M. T., Okaba, D. M., Mostafa, M. S., Mira, H. I., Yang, Z. & El-Sayed, E. T. 2021 Functionalized aminophosphonate chitosan-magnetic nanocomposites for Cd(II) removal from aqueous solutions: performance and mechanisms of sorption. *Appl Surf Sci* **561**. https://doi.org/10.1016/j.apsusc.2021.150069.

Ni, B. J., Huang, Q. S., Wang, C., Ni, T. Y., Sun, J. & Wei, W. 2019 Competitive adsorption of heavy metals in aqueous solution onto biochar derived from anaerobically digested sludge. *Chemosphere* **219**, 351–357. https://doi.org/10.1016/j.chemosphere.2018.12.053.

Noor, I. E., Martin, A. & Dahl, O. 2020 Water recovery from flue gas condensate in municipal solid waste fired cogeneration plants using membrane distillation. *Chem Eng J* **399**. https://doi.org/10.1016/j.cej.2020.125707.

Öman, C., Malmberg, M. & Wolf-Watz, C. 2000 Handbook for leachate assessment, method for characterization of leachate from waste sites [Handbok för Lakvattenbedömning, Metodik för karakterisering av lakvatten från avfallsupplag] [WWW Document]. Available from: https://www.ivl.se/download/18.34244ba71728fcb3f3f5c3/1591704226532/B1354.pdf (accessed 5 June 2023).

Özer, A. & Tümen, F. 2003 Cd(II) adsorption from aqueous solution by activated carbon from sugar beet pulp impregnated with phosphoric acid. *Fresenius Environ Bull* **12**, 1050–1058.

Rangabhashiyam, S., dos Santos Lins, P. V., de Magalhães Oliveira, L. M., Sepulveda, P., Ighalo, J. O., Rajapaksha, A. U. & Meili, L. 2022 Sewage sludge-derived biochar for the adsorptive removal of wastewater pollutants: a critical review. *Environ Pollut* **293**. https://doi.org/10.1016/j.envpol.2021.118581.

Renström, T. 2018 *Mapping Metalflows in Wastewater in Västerås [Kartläggning av metallflöden i avloppsvatten i Västerås]*. Master Thesis. Uppsala University, Uppsala.

Ruffino, B., Campo, G., Genon, G., Lorenzi, E., Novarino, D., Scibilia, G. & Zanetti, M. 2015 Improvement of anaerobic digestion of sewage sludge in a wastewater treatment plant by means of mechanical and thermal pre-treatments: performance, energy and economical assessment. *Bioresour Technol* **175**, 298–308. https://doi.org/10.1016/j.biortech.2014.10.071.

Ruffino, B., Cerutti, A., Campo, G., Scibilia, G., Lorenzi, E. & Zanetti, M. 2020 Thermophilic vs. mesophilic anaerobic digestion of waste activated sludge: modelling and energy balance for its applicability at a full scale WWTP. *Renew Energy* **156**, 235–248. https://doi.org/10.1016/j.renene.2020.04.068.

Salman, C. A., Schwede, S., Thorin, E., Li, H. & Yan, J. 2019 Identification of thermochemical pathways for the energy and nutrient recovery from digested sludge in wastewater treatment plants. *Energy Procedia* **158**, 1317–1322. https://doi.org/10.1016/j.egypro.2019.01.325.

Sartz, L. & Bäckström, M. 2013 Treatment of acidic and neutral metal-laden mine waters with bone meal filters. *Mine Water Environ* **32**, 293–301. https://doi.org/10.1007/s10230-013-0248-2.

Sizmur, T., Fresno, T., Akgül, G., Frost, H. & Moreno-Jiménez, E. 2017 Biochar modification to enhance sorption of inorganics from water. *Bioresour Technol* **246**, 34–47. https://doi.org/10.1016/j.biortech.2017.07.082.

Sörme, L. & Lagerkvist, R. 2002 Sources of heavy metals in urban wastewater in Stockholm. *Sci Total Environ* **298**, 131–145. https://doi.org/10.1016/S0048-9697(02)00197-3.

Sylwan, I. & Thorin, E. 2021 Removal of heavy metals during primary treatment of municipal wastewater and possibilities of enhanced removal: a review. *Water (Basel)* **13**. https://doi.org/10.3390/w13081121.

Sylwan, I. & Thorin, E. 2023 Potential of sludge-derived char as a metal sorbent during primary settling of municipal wastewater. *Environ Technol Innov* **32**, 103258. https://doi.org/10.1016/j.eti.2023.103258.

Tao, H., Zhang, H., Li, J. & Ding, W. 2015 Biomass based activated carbon obtained from sludge and sugarcane bagasse for removing lead ion from wastewater. *Bioresour Technol* **192**, 611–617. https://doi.org/10.1016/j.biortech.2015.06.006.

Tchounwou, P. B., Yedjou, C. G., Patlolla, A. K. & Sutton, D. J., 2012 Heavy metal toxicity and the environment. In: *Molecular, Clinical and Environmental Toxicology* (Luch, A, ed.). Springer, Basel, pp. 133–164. https://doi.org/10.1007/978-3-7643-8340-4_6.

Tran, H. N., You, S. J., Hosseini-Bandegharaei, A. & Chao, H. P. 2017 Mistakes and inconsistencies regarding adsorption of contaminants from aqueous solutions: a critical review. *Water Res* **120**, 88–116. https://doi.org/10.1016/j.watres.2017.04.014.

Wang, Z., Chen, D., Song, X. & Zhao, L. 2012 Study on the combined sewage sludge pyrolysis and gasification process: mass and energy balance. *Environ Technol* **33**, 2481–2488. https://doi.org/10.1080/09593330.2012.683816.

Wongrod, S., Simon, S., van Hullebusch, E. D., Lens, P. N. L. & Guibaud, G. 2018 Changes of sewage sludge digestate-derived biochar properties after chemical treatments and influence on As(III and V) and Cd(II) sorption. *Int Biodeterior Biodegradation* **135**, 96–102. https://doi.org/10.1016/j.ibiod.2018.10.001.

Xiang, W., Zhang, X., Chen, J., Zou, W., He, F., Hu, X., Tsang, D. C. W., Ok, Y. S. & Gao, B. 2020 Biochar technology in wastewater treatment: a critical review. *Chemosphere* **252**, 126539. https://doi.org/10.1016/j.chemosphere.2020.126539.

Xu, X., Zhao, Y., Sima, J., Zhao, L., Masek, O. & Cao, X. 2017 Indispensable role of biochar-inherent mineral constituents in its environmental applications: a review. *Bioresour Technol* **241**, 887–899. https://doi.org/https://doi.org/10.1016/j.biortech.2017.06.023.

Zhai, Y., Wei, X., Zeng, G., Zhang, D. & Chu, K. 2004 Study of adsorbent derived from sewage sludge for the removal of Cd^{2+}, Ni^{2+} in aqueous solutions. *Sep Purif Technol* **38**, 191–196. https://doi.org/10.1016/j.seppur.2003.11.007.

Zhang, W., Mao, S., Chen, H., Huang, L. & Qiu, R. 2013 Pb(II) and Cr(VI) sorption by biochars pyrolyzed from the municipal wastewater sludge under different heating conditions. *Bioresour Technol* **147**, 545–552. https://doi.org/10.1016/j.biortech.2013.08.082.

First received 31 July 2023; accepted in revised form 31 October 2023. Available online 9 November 2023